Hindawi Publishing Corporation
Advances in Materials Science and Engineering
Volume 2013, Article ID 987572, 8 pages
http://dx.doi.org/10.1155/2013/987572

Research Article

Nonlinear-Electronic Transport in Fe_2O_3 Thin-Films Grown from Grain-Oriented Iron Foils

Roberto Baca Arroyo

Department of Electronics, National Polytechnic Institute, Distrito Federal, Mexico City 07738, MEX, Mexico

Correspondence should be addressed to Roberto Baca Arroyo; rbaca02006@yahoo.com.mx

Received 16 August 2013; Accepted 24 October 2013

Academic Editor: Feng Zhao

Nonlinear-electronic transport in Fe_2O_3 thin-films grown by thermal oxidation from grain-oriented iron foils was studied by current-voltage characteristics at room temperature as a function of the oxidation temperature. Microstructure formation and its changes were investigated by atomic force microscopy and X-ray diffraction studies. X-ray diffraction has demonstrated that average grain size was weakly increased with the growth temperature. The analysis of current-voltage characteristics shows ohmic regime at low voltages and space-charge-limited regime at higher voltages. Space-charge effects resulted from the discontinuous grain growth of the foils. Further, nonlinear-electronic transport of Fe_2O_3 thin-films can be useful for the designing of adaptive oxide electronic devices.

1. Introduction

Space-charge-limited current was studied in vacuum tube technology at around 1906. Scientists had developed technologies based on vacuum tubes including high-power, signal amplifier, and military applications, due to its resistance to electromagnetic pulse. Therefore, the space charge phenomena can renewal the era of solid-sate-electronics in the operation principle of adaptive oxide electronic devices based on space-charge effects, which could be useful for smart devices with nonlinear characteristics [1–3].

Recently was demonstrated how changing from bulk to nanoscale materials can significantly change the material properties in transition metal oxides (TMOs) [4] and consequently their performance. Therefore, space-charge effects at the interface between small particles can result in substantial improvement of the electrical, magnetic, and optical properties [5–7].

Adaptive oxide electronic devices based on vertical structure with small area can be implemented in driver circuits for power applications [8, 9], because the current flow can be modulated by an electrode embedded in the middle of the device even for low carrier mobility of the metal oxide thin-films [7, 10]. Also, in response to the needs of ecological concerns, low-cost, abundance, stability, nontoxicity, and environmentally, TMOs should be studied and adapted for new applications. For example, iron oxide has attracted interest of researchers [11–13]. It is well known that hematite (Fe_2O_3) has a low conductivity as well as low electron mobility at room temperature in comparison with silicon [14]. Also, it is known that activation energy for Fe_2O_3 varies nonmonotonically with temperature [15, 16].

Nonlinear-electronic transport in Fe_2O_3 thin-films produced by thermal oxidation has been investigated in this work. Microstructure formation was studied by atomic force microscopy and X-ray diffraction as a function of the growth temperature as well as the study of the nonlinear-current conduction as a function of thickness was conducted by current-voltage characteristics at room temperature.

2. Experimental Procedure

Fe_2O_3 thin-films were grown by thermal oxidation from grain-oriented iron foils. The grain-oriented iron foil is a soft magnetic material that is used as the core material in electrical transformers. In this work, grain-oriented foils were obtained from cores of low-power transformers with thickness of

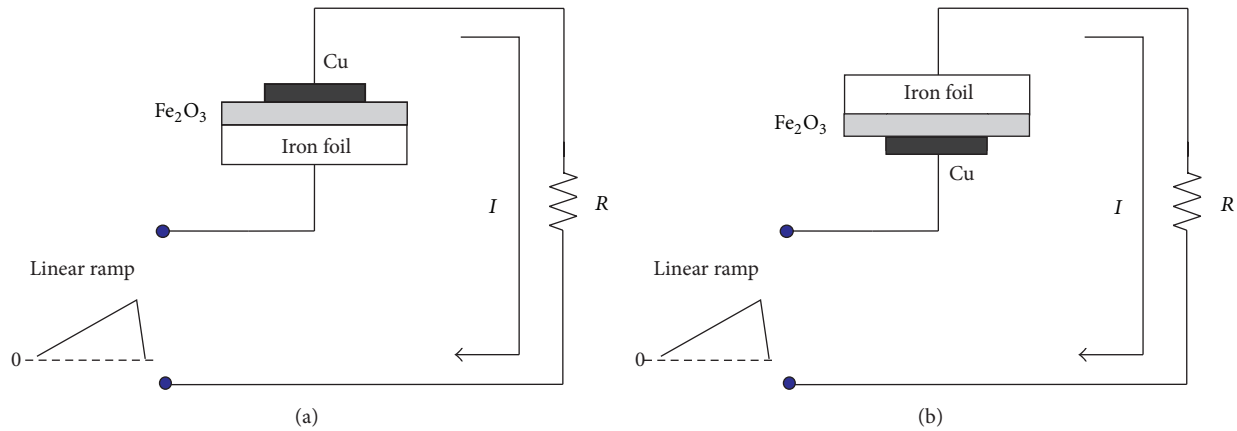

Figure 1: Schematic diagram of samples and series circuit under forward bias (a) and reverse bias (b).

0.18 mm. It is known that grain-oriented foils are usually coated to reduce the eddy currents and to provide resistance to corrosion. Therefore, before oxidation processes, the iron foils with cross-sectional area of 1 cm^2 were mechanically polished and cleaned using organic solvents and deionized water. After polishing, the samples were thermally oxidized under air atmosphere conditions in the temperature range from 400°C to 550°C with duration of 20 min into resistively heated quartz tube furnace. A copper electrode of square geometry of 0.1 cm × 0.1 cm was placed on each sample as mechanical point contact as shown in the schematic diagram of Figure 1.

Microstructure formation was analyzed by both atomic force micrographs and X-ray diffraction patterns. Atomic force micrographs of the Fe_2O_3 thin-films were obtained with a Digital Instrument (Veeco) Nanoscope and X-ray diffraction patterns with a PANalytical X-ray diffractometer with CuK_α radiation (λ = 0.15418 nm) in the scan range 20–90°. Current-voltage characteristics of the samples were measured by using digital storage oscilloscope (Tektronix, TDS1012C). Both voltage and current signals were recorded employing a series circuit shown in Figure 1(a) under forward bias and Figure 1(b) under reverse bias. Both voltage and current signals were plotted as lissajous figures on the screen of oscilloscope. A lissajous figure gives the instantaneous values of voltage as a function of the current.

3. Results and Discussion

It is known that the oxidation process of iron oxide should be dependent on the solubility of oxygen into iron foil and energy to take an oxygen ion and form the oxide. Therefore, vacant cation sites (oxygen ions) will diffuse away from the oxide-air interface and vacant anion sites (iron ions) through the oxide during the oxidation process [17]. In the procedure presented here at intermediate temperature (<700°C), a first monolayer of iron oxide is grown and corresponds to Fe_2O_3 phase with lattice parameter similar to grain-oriented iron foil. This phase is characterized by a Goss texture with a (110) preferred crystal orientation [18].

Then, the oxide continues to grow with this texture with strong cohesive forces [17, 19]. Structural defects can be formed into the grown oxide by discontinuous Goss grain growth, which is depending on the industrial production process of the grain-oriented iron foils.

3.1. Microstructure Formation. Microstructure formation studies are conducted to know the stability of the Fe_2O_3 thin-films grown by thermal oxidation at lower temperature than 700°C and under air atmosphere conditions. Atomic force microscopy studies were done to demonstrate the homogeneity and reproducibility of the samples controlled by diffusion process and X-ray diffraction analysis to show the polycrystalline Fe_2O_3 phase formation in the samples.

Figure 2 shows the atomic force micrographs of Fe_2O_3 thin-films at various temperatures. A noncontact mode of operation was employed between the tip and sample with scanned area of 1 μm × 1 μm to provide a method to analyze the oxide formation on samples surface as a function of the roughness based on bearing algorithm from Veeco Nanoscope software.

The average roughness, R_{avg}, can be estimated with the intersection of both depth profile and bearing area plots as indicated in Figure 3 with dashed lines and is related to average grain height distribution, and their values are presented in Table 1.

It is demonstrated that a discontinuous growth mechanism favors the oxide formation and grain size in the samples as shown in Figure 3. However, at temperatures (>500°C), a decrease of the oxide formation can be observed in Figure 3(d), because the discontinuous oxide achieves its critical thickness [17, 18, 20].

Figure 4 shows X-ray diffraction patterns of the thermally oxidized samples. Samples were processed at 400°C and 450°C with peaks located at 65.08° and 81.07° with (530) and (710) planes. Samples were processed at 500°C with peaks located at 30.06°, 35.46°, 43.02°, 65.04°, and 81.07° corresponding to (220), (311), (400), (530), and (710) planes as well as peaks positioned at 33.13°, 35.53°, 42.98°, 65.04°, and 81.07° with (310), (311), (400), (530), and (710) planes

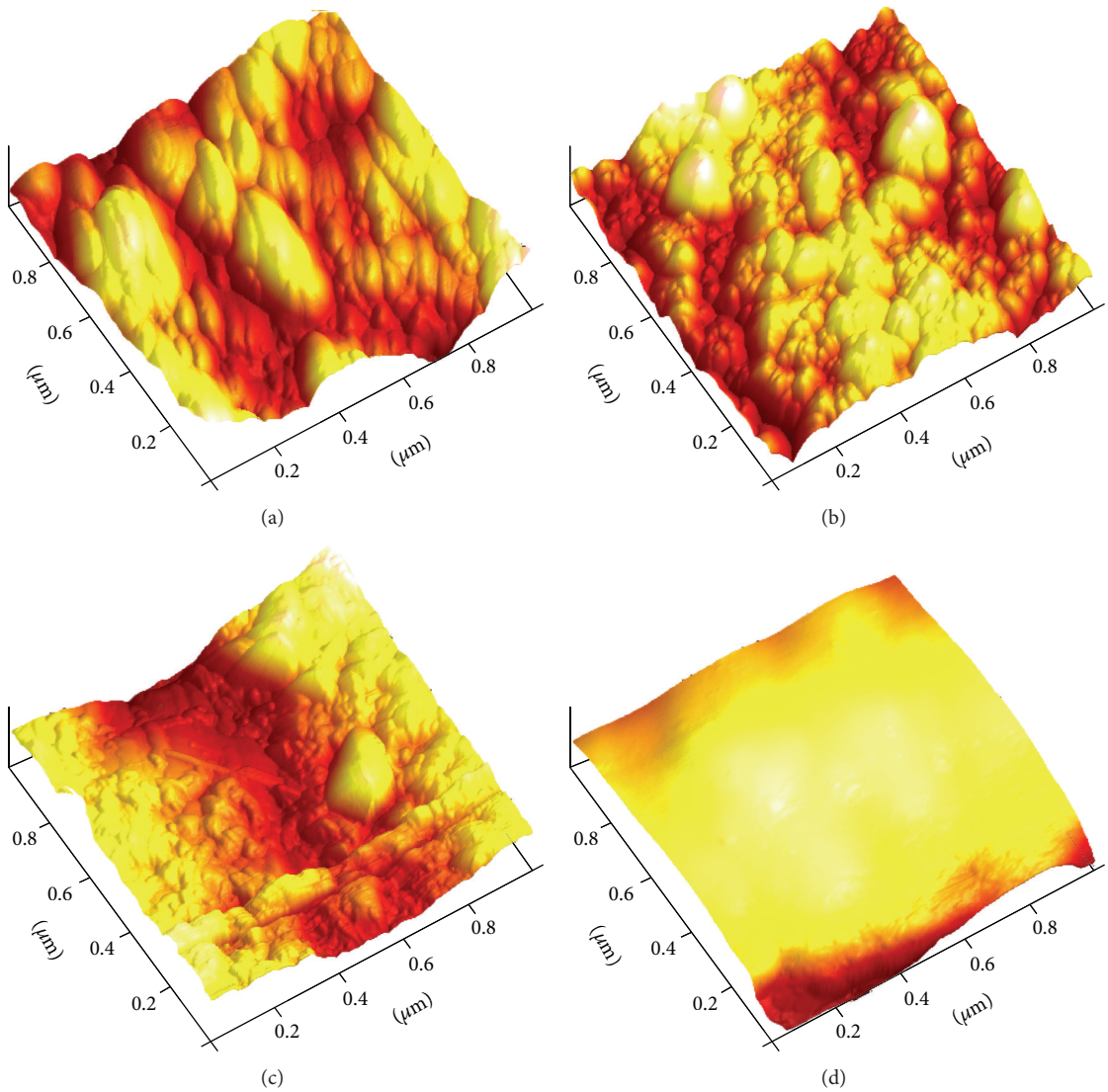

Figure 2: Atomic force micrographs of the oxidized samples under air atmosphere conditions.

were observed in samples processed at 550°C. All peaks correspond to the cubic Fe_2O_3 phase according to PANalytical Card no. 00-019-0629. The cubic Fe structure can be seen in all samples processed with peaks at 44.67° and 82.33° with (110) and (211) planes according to PANalytical Card no. 00-002-0426 and associated with Goss texture [18].

The thickness d of samples was measured by a Tencor profilometer. Both thickness d and average grain size D were indicated in Table 1. Average grain size was estimated with Debye-Scherrer formula based on X-ray diffraction patterns [21, 22].

According to atomic force microscopy studies of Figure 3 and X-ray diffraction analysis of Figure 4, the main scattering mechanism for carries in Fe_2O_3 thin-films can be grain boundary scattering, which is associated with transitional regions between different orientations of neighboring crystallites. Also, potential barrier between crystallites with lattice defects-induced trapping states can impede the carrier motion into the Fe_2O_3 thin-films. As a consequence, when the mean free path of carriers is comparable with smaller crystalline sizes, D, and critical thickness, d, the charge carrier mobility, μ, could be limited according to microstructure data of Table 1 for Fe_2O_3 thin-films.

3.2. Electronic Transport. The performance of samples was demonstrated with the schematic diagram of Figures 1(a) and 1(b). To ensure the linear response, a function generator (Matrix, MFG-8250A) was used to produce a linear ramp signal at low frequency ($f = 100$ Hz) with voltage range from 0 V to 5 V to conserve low-voltage operation and avoid magnetic transport (exchange polarization) in the samples [23, 24]. Also, a resistor of $R = 100\ \Omega$ was selected to monitor the current signal in the samples as shown in Figures 1(a) and 1(b). Current-voltage characteristics for both forward

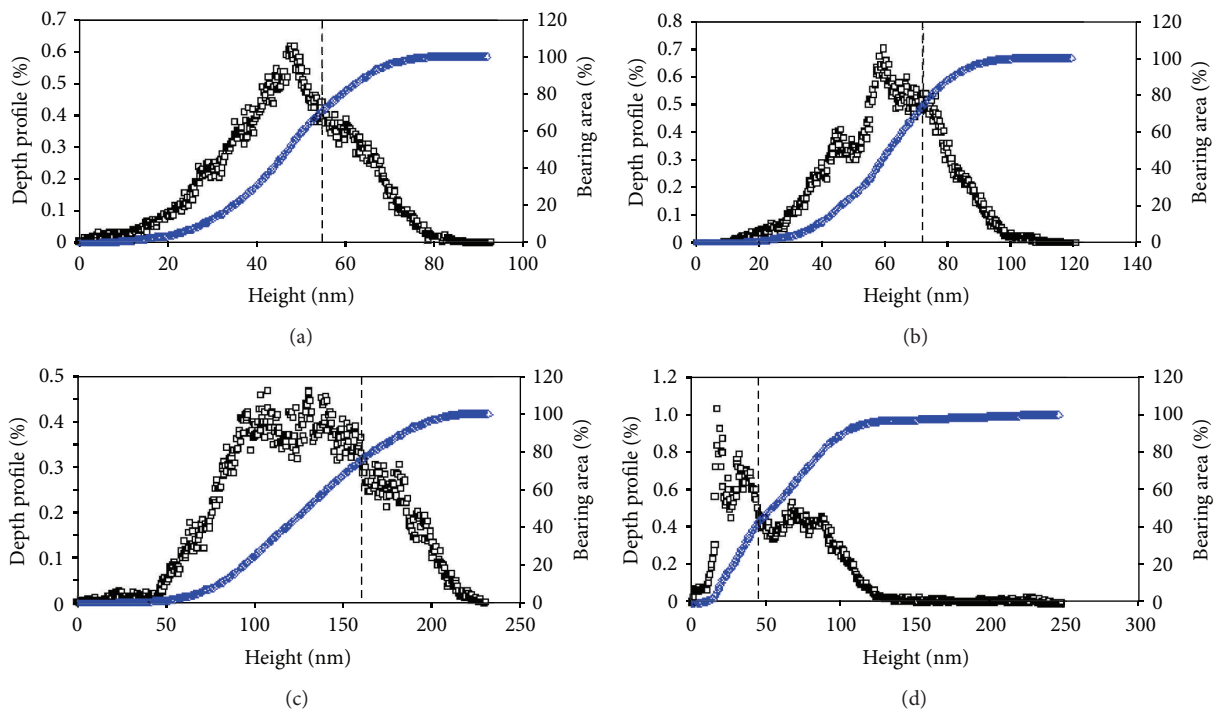

Figure 3: Depth profile and bearing area plots of the analyzed micrographs of Figure 2.

Table 1: Microstructure data for Fe_2O_3 thin-films.

Sample	T (°C)	d (nm)	R_{avg} (nm)	D (nm)
a	400	150	27.5	22.8
b	450	165	36.1	29.3
c	500	220	81.2	21.9
d	550	255	21.8	34.2

and reverse bias are shown in Figures 5 and 6. Nonlinear-electronic transport was observed on the current-voltage characteristics with two regions indicated by slopes.

To investigate the transport parameters of the samples, a model of space-charge-limited transport was proposed and given by

$$I = \frac{9}{32\pi}\varepsilon\mu A_e \frac{N_c}{N_t} \exp\left(-\frac{\phi_t}{k_B T}\right)\frac{V^n}{d^3}, \quad (1)$$

where ε is the iron oxide dielectric constant (taken as $\varepsilon = 540$ for Fe_2O_3 at low frequencies) [15], k_B is the Boltzmann constant, T is the sample temperature, μ is the charge carrier mobility, A_e is the effective cross-sectional area ($A_e = 1\ \text{cm}^2$), N_c is the density of the states available ($N_c = 1.35 \times 10^{19}\ \text{cm}^{-3}$) [14], N_t is the density of traps, ϕ_t is the energy level of the traps, V is the applied voltage, and d is the thickness of the Fe_2O_3 thin-films.

The trap concentration, N_t, was estimated from the current-voltage characteristics, with the voltage which is related to slope change and that intersects to the potential drop, V_{TFL}, across the films as indicated in both Figures 5 and 6 [25]. As shown in Figures 5 and 6, ohmic regime $I \propto V$ was observed at low voltages ($0 < V < V_{TFL}$), while at higher voltages ($V_{TFL} < V < 5V$), with $I \propto V^n$ regime for $n = 1.5$ to 2. The parameter V_{TFL} corresponds to voltage associated with trap-filled limit with charge carriers and can be linked with the following relation:

$$N_t = \frac{\varepsilon}{6e}\frac{V_{TFL}}{d^2}. \quad (2)$$

Nonlinear behavior on current-voltage characteristics was observed in Figures 5 and 6, which can be associated with collision-free transport at low voltages and collision-dominated transport at higher voltages [26]. It is known that collision-free transport associated with low-field transport is influenced by weak thermal vibrations and charge carrier mobility, μ, independent of the field because carries and lattice are in equilibrium. However, under transport at higher voltages, the collision-dominated transport becomes a nonlinear function of carries with the field and charge carrier mobility, μ, into Fe_2O_3 thin-films [27].

Due to the fact that the charge carrier mobility in the space-charge-limited regime, μ_{SCL}, is connected to nonlinear-electronic transport of the samples, the value of μ_{SCL} should be evaluated for the designing of adaptive electronic devices. μ_{SCL} can be estimated from $\Delta I = ne\mu A_e \Delta V d^{-1}$ as

$$\mu_{SCL} = \frac{d}{N_t e A_e} m, \quad (3)$$

where m is first slope (ohmic region) on the current-voltage characteristics of Figures 5 and 6 and was extracted using $m = \Delta I/\Delta V$, with ΔI as the differential change of current and ΔV as the differential change of voltage, respectively.

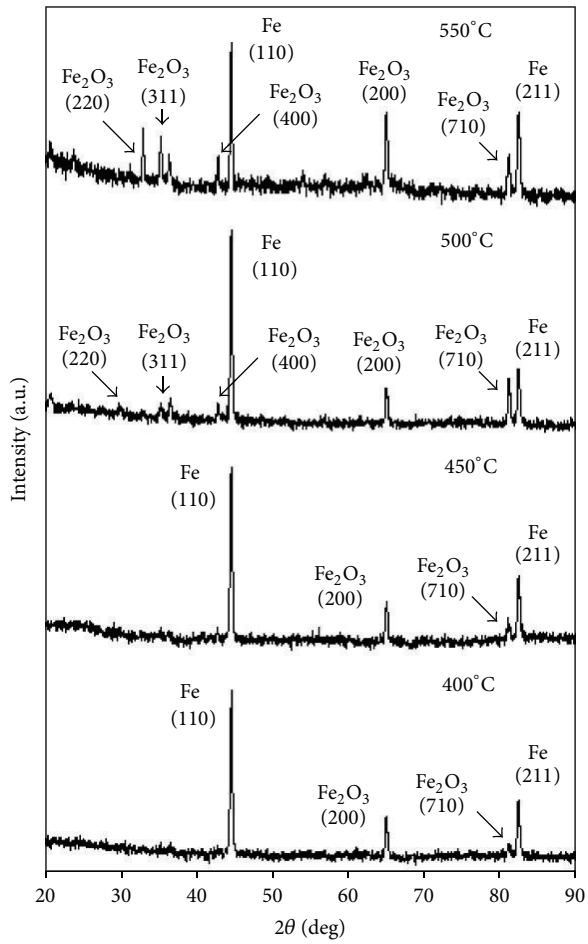

Figure 4: XRD patterns of the oxidized samples under air atmosphere conditions.

Table 2: Transport parameters under forward bias.

Sample	V_{TFL} (V)	N_t (cm^{-3})	m	μ_{SCL} ($cm^2\,V^{-1}\,s^{-1}$)	α	ϕ_t (eV)
a	1.2	2.4×10^{15}	6.5×10^{-3}	0.26×10^{-3}	1.5×10^{-3}	0.36
b	0.8	1.3×10^{15}	7.5×10^{-3}	0.59×10^{-3}	3.3×10^{-3}	0.37
c	1.1	9.9×10^{14}	5.7×10^{-3}	0.78×10^{-3}	2.7×10^{-3}	0.37
d	1.6	1.1×10^{15}	3.4×10^{-3}	0.48×10^{-3}	1.1×10^{-3}	0.36

It is assumed in (3) that m can be extracted from ohmic region because low-field transport is used in characterizing semiconductor films to determine the concentration of thermally excited carries, n, and its charge carrier mobility, μ, [26]. Thus, under space-charge-limited regime, $N_t \gg n$ and (3) with $n = N_t$ was solved.

The space-charge-limited regime obeys to $I = \alpha V^n d^{-3}$, where α is a scaling factor which depends on ε, μ, and N_c/N_t ratio. According to (1), α is expressed by

$$\alpha = \frac{9}{32\pi}\varepsilon\mu A_e \frac{N_c}{N_t} \exp\left(-\frac{\phi_t}{k_B T}\right). \quad (4)$$

Therefore, transport parameters of the Fe_2O_3 thin-films were extracted solving (2), (3), and (4) and using MATLAB program. Parameter α was estimated based on nonlinear behavior of Figures 5 and 6 and energy level of traps, ϕ_t, was calculated from (4). Finally, transport parameters were listed for both forward and reverse bias in Tables 2 and 3, respectively.

From Tables 2 and 3, it was demonstrated that activation energy, ϕ_t, for Fe_2O_3 layers varies nonmonotonically with temperature. The V_{TFL} parameter was different for the samples, because slope changes were observed into the current-voltage characteristics, which is related to traps concentration changes, N_t, during the formation of discontinuous Fe_2O_3 thin-films. Contact effects of both Fe/Fe_2O_3 and Fe_2O_3/Cu interfaces may also influence device performance, because grain boundary scattering related with lattice defects-induced

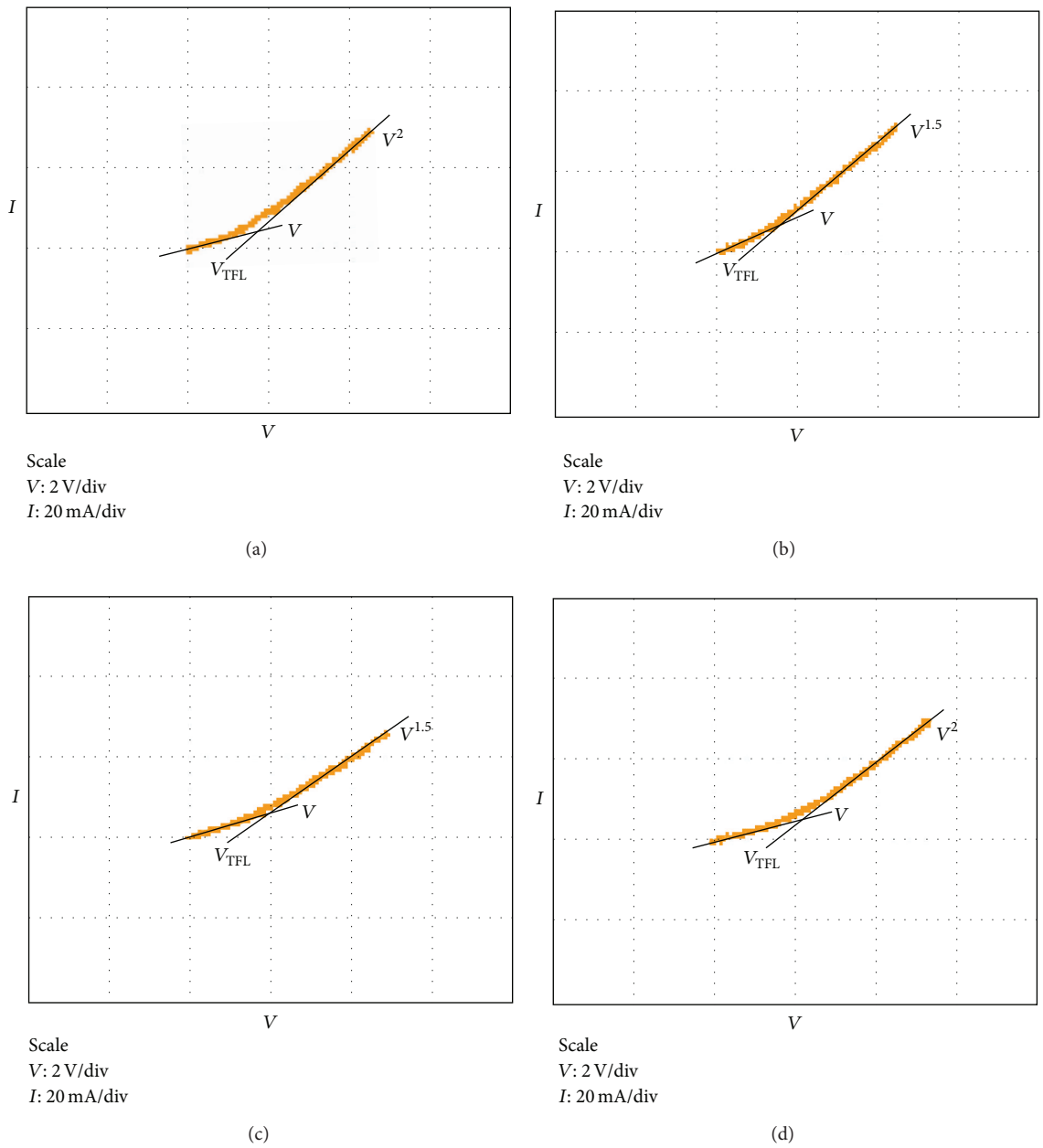

Figure 5: Current-voltage characteristics under forward bias.

Table 3: Transport parameters under reverse bias.

Sample	V_{TFL} (V)	N_t (cm^{-3})	m	μ_{SCL} ($cm^2\,V^{-1}\,s^{-1}$)	α	ϕ_t (eV)
a	0.8	1.5×10^{15}	2.5×10^{-3}	0.15×10^{-3}	3.0×10^{-3}	0.34
b	1.6	2.7×10^{15}	3.0×10^{-3}	0.11×10^{-3}	1.0×10^{-3}	0.34
c	1.8	1.6×10^{15}	3.1×10^{-3}	0.26×10^{-3}	9.6×10^{-3}	0.35
d	1.1	7.7×10^{14}	3.7×10^{-3}	0.77×10^{-3}	2.8×10^{-3}	0.36

trapping states near to the interface impedes the charge carrier motion by space-charge phenomena.

Nonlinear-electronic transport in samples with lower critical thickness of 250 nm varies monotonically with the low charge carrier mobility, μ_{SCL}, in the space-charge-limited regime [8, 25]. The low charge carrier mobility in Tables 2 and 3 was affected by bias because the Fe_2O_3 phase provides strong cohesive forces with iron foil and allows a carriers transport with increase of μ_{SCL} under forward bias. However, because structural defects are formed into Fe_2O_3 thin-films

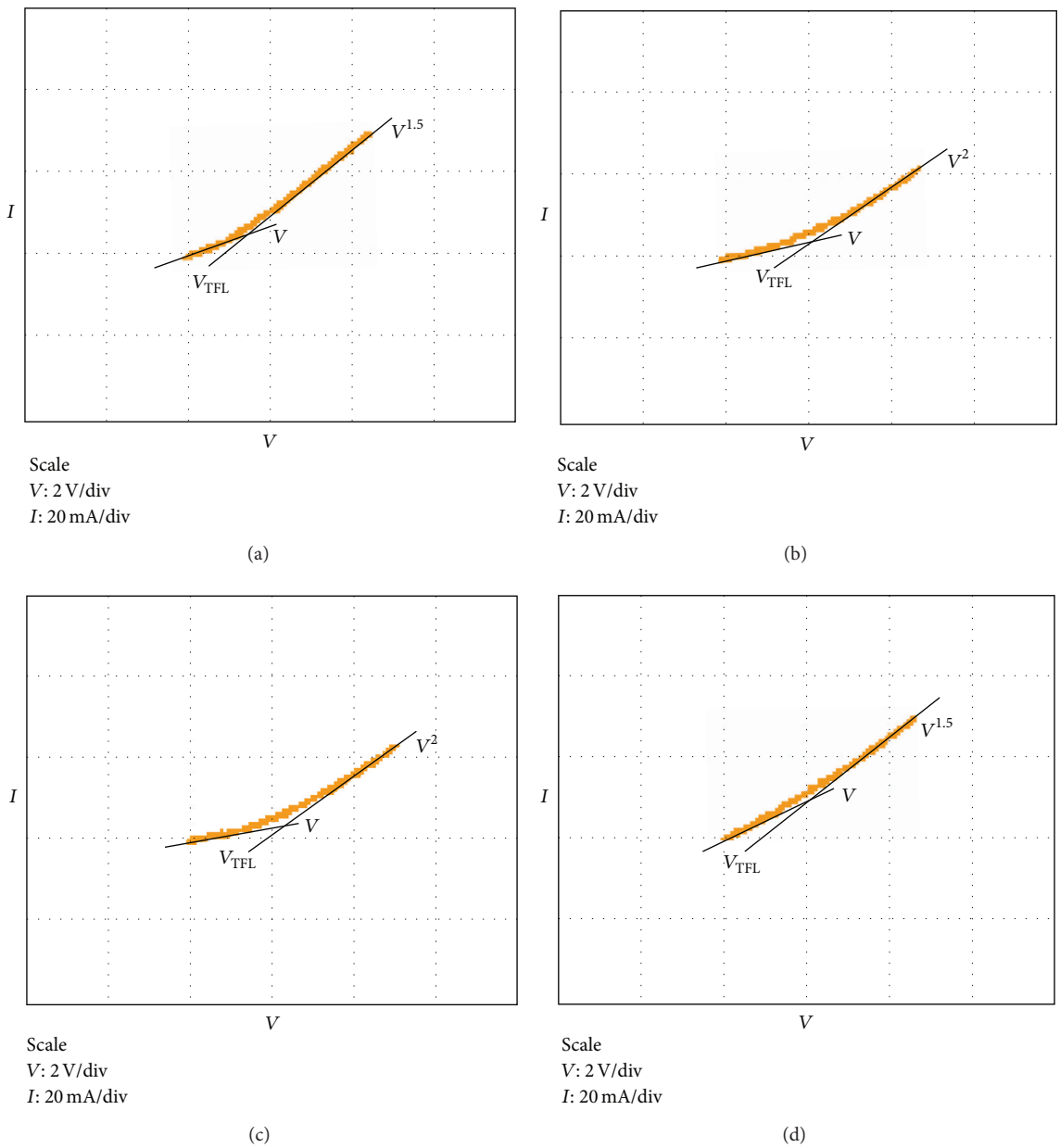

Figure 6: Current-voltage characteristics under reverse bias.

during the oxidation process, weak cohesive forces between Fe_2O_3 phase and copper contact allow a carriers transport with decrease of μ_{SCL} under reverse bias. Finally, increase of average roughness, R_{avg}, and smaller crystalline size, D, in correlation with changes of charge carrier mobility, μ_{SCL}, is a consequence of space-charge-limited transport in Fe_2O_3 thin-films.

4. Conclusion

Nonlinear-electronic transport from Fe_2O_3 thin-films was studied by current-voltage characteristics as a function of the oxidation temperature. Both average roughness and grain size were demonstrated by atomic force microscopy and X-ray diffraction studies. Transport parameters were evaluated for all samples at room temperature. Space-charge effects were related to the formation of discontinuous oxide based on discontinuous grain growth during the oxidation process at intermediate temperatures. Analysis of current-voltage characteristics shows ohmic regime at low voltages and space-charge-limited regime at higher voltages.

Further, the iron oxide samples with lower critical thickness of 250 nm can be useful for the designing of adaptive oxide electronic devices, because the current flow in the Fe_2O_3 thin-films with low carrier mobility and low energy level of the traps, can be gradually modulated.

Conflict of Interests

The author declares that there is no conflict of interests, such as financial gain, but there is a direct interest regarding the publication of this paper to share knowledge in this area.

Acknowledgments

The process and results obtained in this work have been possible thanks to the previous support of Dr. Ramón Peña Sierra from CINVESTAV-IPN and Dr. Juan Vicente Méndez Méndez from CNMN-IPN, Mexico.

References

[1] Y.-C. Chao, M.-C. Ku, W.-W. Tsai et al., "Polymer space-charge-limited transistor as a solid-state vacuum tube triode," *Applied Physics Letters*, vol. 97, no. 22, Article ID 223307, 2010.

[2] S. Brimley, M. S. Miller, and M. J. Hagmann, "Field emission in air and space-charge-limited currents from iridium-iridium oxide tips with gaps below 100 nm," *Journal of Applied Physics*, vol. 109, no. 9, Article ID 094510, 2011.

[3] J. Kim, K. No, and C. J. Lee, "Growth and field emission of carbon nanotubes on electroplated Ni catalyst coated on glass substrates," *Journal of Applied Physics*, vol. 90, no. 5, pp. 2591–2594, 2001.

[4] J. Cao and J. Wu, "Strain effects in low-dimensional transition metal oxides," *Materials Science and Engineering R*, vol. 71, no. 2–4, pp. 35–52, 2011.

[5] C.-Y. Chen, Y.-C. Chao, H.-F. Meng, and S.-F. Horng, "Light-emitting polymer space-charge-limited transistor," *Applied Physics Letters*, vol. 93, no. 22, Article ID 223301, 2008.

[6] A. S. Aricò, P. Bruce, B. Scrosati, J.-M. Tarascon, and W. Van Schalkwijk, "Nanostructured materials for advanced energy conversion and storage devices," *Nature Materials*, vol. 4, no. 5, pp. 366–377, 2005.

[7] P. LeMinh, H. Gokcan, J. C. Lodder, and R. Jansen, "Magnetic tunnel transistor with a silicon hot-electron emitter," *Journal of Applied Physics*, vol. 98, no. 7, Article ID 076111, 2005.

[8] P. Kumar, A. Jain, M. Shukla, and S. Chand, "Space charge limited current in Schottky diode with single level traps," *Indian Journal of Pure and Applied Physics*, vol. 49, no. 6, pp. 406–409, 2011.

[9] L. Dulau, S. Pontarollo, A. Boimond, J.-F. Garnier, N. Giraudo, and O. Terrasse, "A new gate driver integrated circuit for IGBT devices with advanced protections," *IEEE Transactions on Power Electronics*, vol. 21, no. 1, pp. 38–43, 2006.

[10] S. A. Moiz, M. M. Ahmed, K. S. Karimov, F. Rehman, and J.-H. Lee, "Space charge limited current-voltage characteristics of organic semiconductor diode fabricated at various gravity conditions," *Synthetic Metals*, vol. 159, no. 13, pp. 1336–1339, 2009.

[11] A. Cotton and G. Wilkinson, *Advanced Inorganic Chemistry*, John Wiley & Sons, New York, NY, USA, 4th edition, 2008.

[12] R. Baca, "Structural characterization of the chromium-iron alloy formed by thermal diffusion processes," *Advanced Materials Research*, vol. 651, pp. 284–288, 2013.

[13] P. Liao and E. A. Carter, "Hole transport in pure and doped hematite," *Journal of Applied Physics*, vol. 112, pp. 1–13, 2012.

[14] R. F. G. Gardner, F. Sweett, and D. W. Tanner, "The electrical properties of alpha ferric oxide—II. Ferric oxide of high purity," *Journal of Physics and Chemistry of Solids*, vol. 24, no. 10, pp. 1183–1186, 1963.

[15] F. J. Morin, "Electrical properties of α-Fe_2O_3," *Physical Review*, vol. 93, no. 6, pp. 1195–1199, 1954.

[16] P. Liao, M. C. Toroker, and E. A. Carter, "Electron transport in pure and doped hematite," *Nano Letters*, vol. 11, no. 4, pp. 1775–1781, 2011.

[17] N. Cabrera and N. F. Mott, "Theory of the oxidation of metals," *Reports on Progress in Physics*, vol. 12, no. 1, pp. 163–184, 1949.

[18] D. Dorner, S. Zaefferer, L. Lahn, and D. Raabe, "Overview of microstructure and microtexture development in grain-oriented silicon steel," *Journal of Magnetism and Magnetic Materials*, vol. 304, no. 2, pp. 183–186, 2006.

[19] A. S. Grove, *Physics and Technology of Semiconductor Devices*, John Wiley & Sons, New York, NY, USA, 1st edition, 1967.

[20] G. Ertl, "Thermodynamics of gas-surface interactions," *Pure & Applied Chemistry*, vol. 61, no. 6, pp. 1001–1007, 1989.

[21] P. F. Fewster, *X-Ray Scattering from Semiconductors*, Imperial College Press, Singapore, 2nd edition, 2003.

[22] H. Kashani, "Structural, electrical and optical properties of zinc oxide produced by oxidation of zinc thin films," *Journal of Electronic Materials*, vol. 27, no. 7, pp. 876–882, 1998.

[23] S. Blundell, *Magnetism in Condensed Matter*, Oxford University Press, Oxford, UK, 2nd edition, 2008.

[24] E. Y. Tsymbal and I. Zutic, *Handbook of Spin Transport and Magnetism*, CRC Press/Taylor & Francis Group, Boca Raton, Fla, USA, 1st edition, 2012.

[25] J. J. O'Dwyer, *The Theory of Electrical Conduction and Breakdown in Solid Dielectrics*, Clarendon Press Oxford, 1st edition, 1973.

[26] M. Lundstrom, *Fundamentals of Carrier Transport*, Cambridge University Press, New York, NY, SA, 2nd edition, 2000.

[27] D. H. Zhang and H. L. Ma, "Scattering mechanisms of charge carriers in transparent conducting oxide films," *Applied Physics A*, vol. 62, no. 5, pp. 487–492, 1996.